# Recurrent Neural Network Models of Urban Mobility

Ziheng Lin, Mogeng Yin, Sidney Feygin, Madeleine Sheehan,
Jean-Francois Paiement, Alexei Pozdnoukhov

**Abstract**

Locational data generated by mobile devices present an opportunity to substantially simplify methodologies and reduce analysis latencies in short-term transportation planning applications. Short-term transportation planning, such as traffic flow management or traffic demand management, requires accurate prediction of daily network congestion levels and the congestion contributors. The existing human mobility models using locational data have focused on predicting next activities, and many models limited the prediction to only temporal features or only spatial features that they cannot be directly applied to such applications. In this paper, we propose a Long Short Term Memory (LSTM) model for learning and predicting human mobility sequences using mobile locational data. Our contributions include: first, we developed the LSTM mobility models that are capable of learning and predicting the entire mobility sequences within a time window of interest; second, we developed the LSTM mobility models that are able to predict activity sequences with activity type choices and explicit spatial-temporal choices; third, the LSTM mobility models are able to capture long-term activity dependencies. Lastly, we demonstrate the capability of the LSTM mobility models for learning and generating mobility sequences with contextual information.

## 1 Introduction

From the exponential growth of on-demand shared ride services like Uber and Lyft to an increased reliance on public transit in the face of environmental concerns over emissions and uncertainty in gas prices, today's transportation policy makers and planners must deal with a rapidly changing urban mobility landscape. Despite methodological and technical advances in survey distribution and processing over the last 20 years [1], improvements in the accuracy of transportation demand prediction models have remained flat [13]. As a consequence, project overruns due to inaccurate economic value appraisals continue to cost taxpayers billions of dollars [26, 6]. Non-invasive, automated, continuous data collection mechanisms are increasingly being used to complement manual survey techniques by improving their statistical representativeness [10]. In particular, large volumes of call detail records (CDRs) from mobile phones have been used to construct individual daily itineraries and train travel activity models using weeks and months of data rather than several days' worth [28]. While applications of mining mobility trajectories from crowd-sourced locational data are common (these are thoroughly reviewed in Section 2), existing models often trade off the interpretability that transportation practitioners require in practice for the computational tractability necessary to deal with large volumes of data [7].

In practice, the activity-based travel models used by practitioners are incredibly rich in describing the intricacies of human activities and context of decision making in travel-related choices. The appeal of econometric models estimated from these stated preference data of transportation system users rests on empirically-validated utility maximization axioms and the estimation of parameters for linear models that explain choices based on the characteristics of individual decision makers and the attributes of the alternatives under consideration [4]. However, it is usually difficult for discrete choice model framework to be generalized for modeling sequential choice involving multiple decisions simultaneously. In computer science community, on the other hand, large amounts of work focus on modeling and predicting human mobility on the individual level, such that the characteristic of individuals are often ignored. Many sequence modeling frameworks such as Markov models and recurrent neural networks have been developed but have not been applied and evaluated on the transportation domain. Thus, one key research challenge for the community in lies in developing a framework that reduces reliance on domain experts to specify robust models of sequential travel

decision-making while maintaining the flexibility to include covariates that rationalize observed behavior and responses to the applied system-level policies.

In this paper, we describe the developed a generative modeling framework that is capable of learning activity sequences from large volumes of call data while incorporating behavioral parameters that are sensitive to policy levers. By combining recurrent neural networks with probabilistic modeling techniques specific to the task of generating human activity chains from cellular data, we thus expand the scope of state-of-the-art human mobility modeling techniques to the realm of decision support for transportation policy analysis. This paper details the following contributions:

- We developed mobility sequence models that are capable of learning and predicting the entire mobility sequences within the time window of interest.
- We developed mobility sequence models that are able to predict activity sequences with activity-type choices and explicit spatial-temporal choices.
- We developed mobility sequence models that are able to capture long-term activity dependencies.
- We developed mobility sequence models that are capable of learning and generating sequences with contextual information.

# 2 Related Work

Enabled by petabyte-scale data processing techniques, urban computing innovations and challenges have been drawing increasing social, commercial, and academic attention in the past decade [32]. Human activity recognition from spatiotemporal microdata streams, an application of urban computing research, has been explored extensively by practitioners across disciplines[14, 7]. A summary of relevant developments in urban activity modelling is given below with respect to the main data sources and the properties of the explored algorithms.

## 2.1 Locational Data Sources

GPS data is granular in both spatial and temporal resolution. Early work in extracting significant places took advantage of this relatively rich data source for activity inference models [33, 20]. However, collecting GPS data often requires active user participation and permissions for physical devices as well as careful battery management, thus limiting its practicality in terms of collecting continuous and representative samples from traveler populations.

Locational-based social network (LBSN) data usually contains locations of users of a service at the time of interaction (a check-in), and is limited by the frequency of users' check-ins. Based on LBSN data, researches have developed methods for classifying activities into distinct categories [29, 19], for separating social trips from commute trips [8], promoting products and services [34] and inferring mobility of grouped individuals [31].

The anonymized Call Detail Records (CDRs) from cellular network operators provide a compromise between spatial-temporal resolution and ubiquity. Due to its relatively poor resolution in space, CDR data has been mainly used to derive spatially aggregated results such as mass movements of population [12], aggregated origin-destination (OD) estimation [27], stylized mobility laws [14, 22], and disaster response [21].

## 2.2 Generative Models for Sequential Data

To a large extent, human mobility is structured by highly regular daily/weekly schedules, demonstrating high predictability across diverse populations [14]. Longitudinal analysis also suggests that human mobility has high temporal and spatial regularities [22]. With the right tools, these patterns can be employed in predictive models.

Hidden (semi-) Markov Models are generative models that can not only be used to analyze patterns in sequences, but also to generate new sequences [17]. Recent work used Input-Output Hidden Markov Models

(IO-HMMs) to reveal urban activity patterns (including the spatial-temporal profiles of urban activity and heterogeneous transition probabilities) and to generate synthetic activity sequences to inform microscopic traffic simulations [30]. The advantage for HMMs is that they are suitable for sequence of arbitrary length, and they are capable for unsupervied learning of sequences. The disadvantage of the HMMs is that they need the manual selection of the number of hidden states; and the contextual variables often need to be carefully crafted in order for the IO-HMMs to perform well.

Recurrent neural networks (RNNs) have become the state of the art for sequence modeling and generation, especially in the language and translation domain [25]. Long short term memory (LSTM) [18] is one of the most popular variations of RNNs with proven ability to generate sequences in various domains, such as text [24], images [16] and hand-writing [15, 9]. Recent works showed the capability of LSTM to predict individual mobilities using GPS data [23] and to predict pedestrians' motion from video data [2]. Another recent work showed the great performance of labeling acoustic and accelerometer sequences using a combination of Hidden Semi-Markov Model and Recurrent Neural Network [11]. The success of RNNs in these domains motivated our work of applying RNNs for human activity sequence modeling and generation. The advantage of LSTM models over HMMs is that the continuous hidden states that gives the flexibility of modeling arbitrary distributions with long-term dependencies.

# 3 Learning Activity Sequences with Long Short-Term Memory (LSTM)

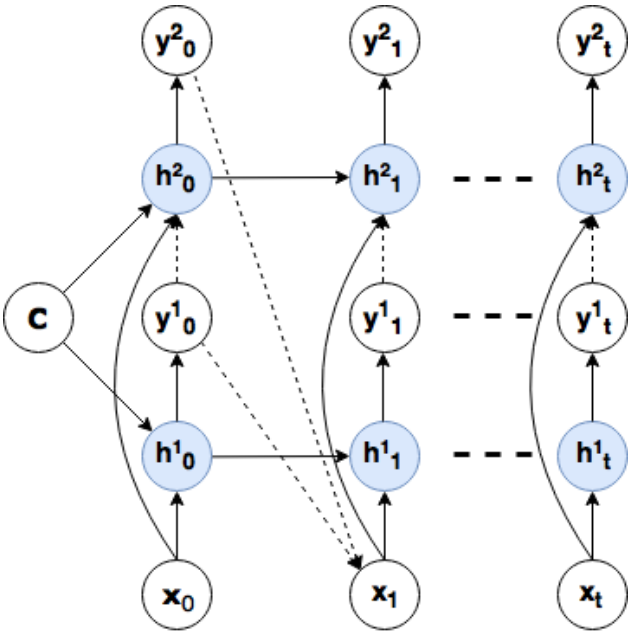


Figure 1: LSTM Model Structure

In this section, we describe the LSTM model structures that generate activity sequences with explicit spatial-temporal choice and activity types, which is shown in Fig 1. We denote the target activity sequences as $S$ and contextual information for the sequences as $c$. There are two layers in the model responsible for learning activity types and spatial-temporal distributions for the next activity given input $x_t$. The contextual information $c$ is passed into both layers only at timestamp 0, while features of previous activity $x_{t-1}$ is passed into both layers at each timestamp, $t$. We employ techniques of mixture density networks (MDNs) [5, 15], for the spatial-temporal distributions. The idea of mixture density output is that a portion of the LSTM output is used as weights of mixtures, and the rest is used to parameterize each mixture component, which is described below in detail. We use $x_t$, $h_t$, and $y_t$ to denote input variables, hidden states of LSTM layers, and outputs from LSTM layer(s) of $t$'th activity of the day, respectively.

To summarize, our model generates activity sequences according to the following four steps:

1. At timestamp 0, include contextual information $c$ into model input.
2. At every step, $t$, the LSTM layer(s) receives a set of inputs $x_t$.
3. The LSTM layer(s) then produce a set of outputs $y_t$, which is used to parametrize a mixture distribution $p(x_{t+1}|y_t)$.
4. A new activity $x_{t+1}$ is sampled from distribution $p(x_{t+1}|y_t)$.

## 3.1 Input and Context Variables

We design the input variables, $x_t$, such that it contains the features that affect the choices of the next activity. Those features include the current time and the type of the previous activity. Current time is a continuous variable, while activity type is a categorical variable. Activity types consist of the labels of each activity including "home" "work," and "others," which are encoded as a one-hot vector. Thus, $x_t$ can be decomposed as the following:

$$x_t = \{\text{start\_time}_t, \text{type}_{t-1}, \text{day\_of\_week}_t\} \tag{1}$$

The context variable $c$ contains characteristics of individuals. We denote it as the following:

$$c = \{\text{Individual characteristics}\} \tag{2}$$

## 3.2 Output Variables and Mixture Distributions

Output variables $y_t$ are decomposed and transformed into coefficients of mixture distribution $p(x_{t+1}|y_t, c_{t+1})$, which is used for generating the next $x_t$. The first layer outputs the categorical distribution which is used for sampling activity types. And the second layer outputs the 2-dimensional mixture Gaussian distribution for sampling activity duration, and a categorical distribution for sampling the location ID of the activity. Hence, the outputs from the two LSTM layers, $y_t^1$ and $y_t^2$, can be split as the following:

$$y_t^1 = \{\hat{p}_{\text{type}}\} \tag{3}$$

$$\begin{aligned} y_t^2 = \{&\hat{\pi}, \hat{\mu}_{\text{lat}}, \hat{\mu}_{\text{lon}}, \hat{\mu}_{\text{st}}, \hat{\mu}_{\text{dur}}, \\ &\hat{\sigma}_{\text{lat}}, \hat{\sigma}_{\text{lon}}, \hat{\sigma}_{\text{st}}, \hat{\sigma}_{\text{dur}}, \hat{\rho}_{\text{st, dur}}\} \end{aligned} \tag{4}$$

Those raw outputs from LSTM are properly transformed before serving as mixture distribution parameters. The component weights $\hat{\boldsymbol{\pi}}$ and probability of activity type within each component are normalized using softmax function. Standard deviations $\hat{\boldsymbol{\sigma}}_\bullet$ are constrained to be non-negative using an exponential function with correlation coefficients, $\hat{\boldsymbol{\rho}}_\bullet$, scaled between $-1$ and 1 using tanh activation functions. The following equations summarize our model:

$$\pi^i = \frac{\exp(\hat{\pi}^i)}{\sum_j^N \exp(\hat{\pi}^j)}; i \in \{1...N\} \tag{5}$$

$$\mu_\bullet = \hat{\mu}_\bullet \tag{6}$$

$$\sigma_\bullet = \exp(\hat{\sigma}_\bullet) \tag{7}$$

$$\rho_\bullet = \tanh(\hat{\rho}_\bullet) \tag{8}$$

$$p_i = \frac{\exp(\hat{p}_i)}{\sum_j \exp(\hat{p}_j)}; i, j \in \{\text{activity types}\} \tag{9}$$

### 3.3 Mixture Distributions

We define the distributions output from the neural network that models activity types, location, start time, and duration. The activity type is modeled by a categorical distribution that is directly parameterized by the first layer output.

$$\begin{aligned} &p(\text{type}_t|y_{t-1}^1) = p_j; \\ &j \in \{\text{activity types}\} \end{aligned} \tag{10}$$

The spatial-temporal variables and activity type variables are all jointly distributed in one mixture distribution. We write the mixture distribution as follows:

$$\begin{aligned} &p(\text{lat}_t,\text{lon}_t,\text{st}_t,\text{dur}_t|y_{t-1}^2) = \\ &\sum_i^N \pi^i p^i(\text{lat}_t,\text{lon}_t,\text{st}_t,\text{dur}_t|\mu_\bullet,\sigma_\bullet,\rho_\bullet,p_\bullet) \end{aligned} \tag{11}$$

We define the following decomposition of the joint distribution. Here we split a single spatiotemporal four-dimensional Gaussian distribution into a two two-dimensional Gaussian distributions for better computation efficiency, with an assumption of independence between the spatial (latitude, longitude) and temporal variables.

$$\begin{aligned} &p^i(\text{lat}_t,\text{lon}_t,\text{st}_t,\text{dur}_t|\mu_\bullet,\sigma_\bullet,\rho_\bullet,p_\bullet) \\ &\stackrel{\text{def}}{=} p^i(\text{lat}_t,\text{lon}_t)p^i(\text{st}_t,\text{dur}_t) \end{aligned} \tag{12}$$

$$p^i(\text{lat}_t,\text{lon}_t) = \mathcal{N}\left(\text{lat}_t,\text{lon}_t \middle| \begin{bmatrix}\mu_{\text{lat}}^i \\ \mu_{\text{lon}}^i\end{bmatrix}, \Sigma_{\text{lat,lon}}^i\right) \tag{13}$$

$$p^i(\text{st}_t,\text{dur}_t) = \mathcal{N}\left(\text{st}_t,\text{dur}_t \middle| \begin{bmatrix}\mu_{\text{st}}^i \\ \mu_{\text{dur}}^i\end{bmatrix}, \Sigma_{\text{st,dur}}^i\right) \tag{14}$$

where

$$\Sigma_{\text{lat,lon}}^i = \begin{bmatrix}\sigma_{\text{lat}}^2 & 0 \\ 0 & \sigma_{\text{lon}}^2\end{bmatrix} \tag{15}$$

$$\Sigma_{\text{st,dur}}^i = \begin{bmatrix}\sigma_{\text{st}}^2 & \sigma_{\text{st}}\sigma_{\text{dur}}\rho_{\text{st, dur}} \\ \sigma_{\text{st}}\sigma_{\text{dur}}\rho_{\text{st, dur}} & \sigma_{\text{dur}}^2\end{bmatrix} \tag{16}$$

### 3.4 Sampling Activities

Starting from $t = 1$, we sample activity type from $p(\text{type}_t|y_{t-1}^1)$ and activity location and duration from $p(\text{lat}_t,\text{lon}_t,\text{st}_t,\text{dur}_t|y_{t-1}^2)$. The starting time of the next activity is updated by adding the sampled duration to the current time that the start time of each activity is observed prior to the sampling. The conditional mixture weights, mean, and variance of activity duration are calculated as below:

$$w^i(\text{st}_t) = \frac{\pi^i\mathcal{N}(\text{st}_t|\mu_{\text{st}},\sigma_{\text{st}})^i}{\sum_j^N \pi^j\mathcal{N}(\text{st}_t|\mu_{\text{st}},\sigma_{\text{st}})^j} \tag{17}$$

Because of the correlation between activity starting time and duration, the mean and standard deviation of activity duration conditioned on the observed starting time, $\text{st}_t$, is expressed as follows:

$$\mu_{\text{dur}|\text{st}_t} = \mu_{\text{dur}} + \frac{\sigma_{\text{dur}}}{\sigma_{\text{st}}}\rho_{\text{st,dur}}(\text{st}_t - \mu_{\text{st}}) \tag{18}$$

$$\sigma_{\text{dur}|\text{st}_t} = \sqrt{(1-\rho_{\text{st,dur}}^2)}\sigma_{\text{dur}} \tag{19}$$

Now we can sample a new activity $x_t$ from the mixture distribution $p(x_t|y_{t-1})$ following Eq. 20 through Eq. 23. First, a mixture component is sampled from the multinomial distribution of mixture weights ( Eq. 17).

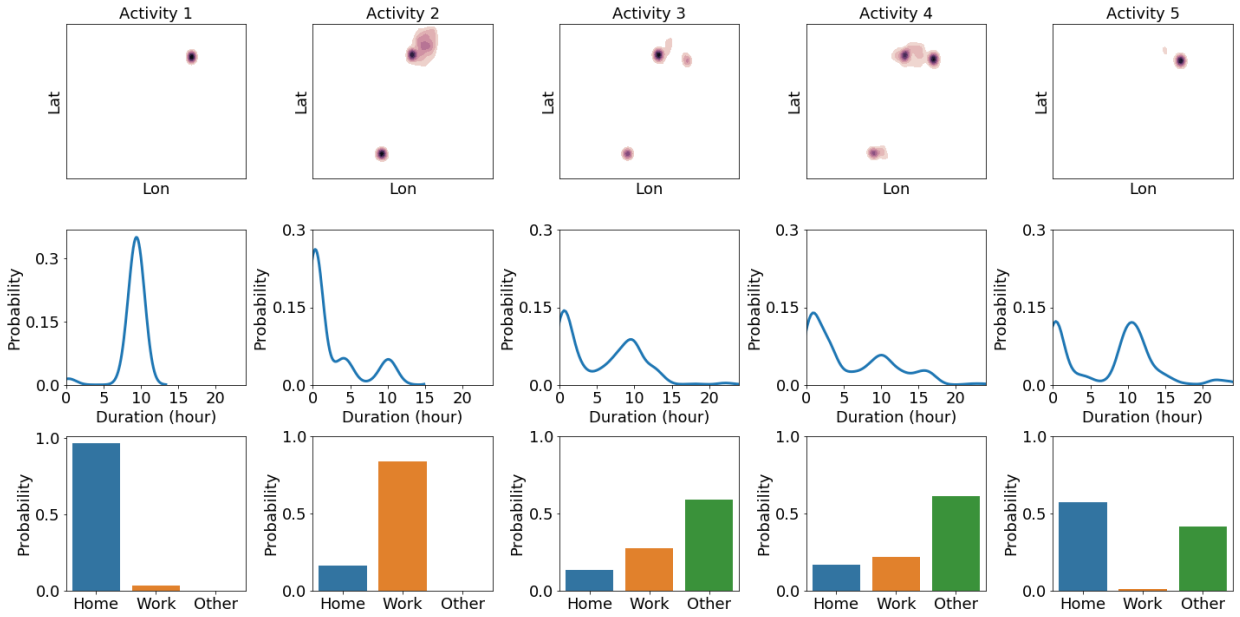


Figure 2: An example of activity sequence generation. Column 1 through 5 represent activities 1 through 5 in a typical day. We can easily notice the home and work location of the artificial individual as well as their corresponding duration. The typical duration of home activities is around 10 hours. The working activities last either under 5 hours or around 10 hours. In this particular day, "home" probability shows highest in the first and last activity; "work" probability shows the highest in the second activity; probability of "other" show the highest in the rest of the activities.

Then, $dur_t$, $lat_t$, $lon_t$ can be further sampled from the selected component, yielding a joint distribution of all those variables. Once a new activity is sampled, the time of day is incremented by $dur_t$.

$$\mathrm{k} \sim \text{Multinomial}\Big(w(\mathrm{st}_t)_1, ..., w(\mathrm{st}_t)_N; n = 1\Big) \tag{20}$$

$$\mathrm{lat}_t, \mathrm{lon}_t \sim \mathcal{N}\left( \begin{bmatrix} \mu^k_{\mathrm{lat}} \\ \mu^k_{\mathrm{lon}} \end{bmatrix}, \Sigma^k_{\mathrm{lat,lon}} \right) \tag{21}$$

$$\mathrm{dur}_t \sim \mathcal{N}\Big(\mu^k_{\mathrm{dur}|\mathrm{st}_t}, \sigma^k_{\mathrm{dur}|\mathrm{st}_t}\Big) \tag{22}$$

$$\mathrm{type}_t \sim \text{Multinomial}\Big(p^k_{\mathrm{home}}, p^k_{\mathrm{work}}, p^k_{\mathrm{others}}; n = 1\Big) \tag{23}$$

In Fig 2, we show an example of the LSTM model generating an activity sequence. The columns represent different activities and the rows represent the spatial-temporal distributions and activity type distributions. Note that we train the LSTM model using an small artificial data set.

## 3.5 Loss Function and Model Estimation

We use negative log-likelihood as the loss of the model. The LSTM model is parameterized by $\theta$. Thus, we propose to directly maximize the probability of the activity sequences given the contextual information by using the following:

$$\theta* = \arg\max_{\theta} \sum_{S,c} \log p(S|c;\theta) \tag{24}$$

We denote the activity at timestamp $t$ along the activity sequence $S$ as $S_t$. We limited the maximum number of activities in a sequence to be T. The joint probability of over $S_1$ ... $S_T$ can be expressed as following:

$$\log p(S|c) = \sum_{t=0}^{T} \log p(S_t|c, S_1...S_{t-1}) \tag{25}$$

The output from the neural network $y_t$ carries information accumulated in the neural network memory from all previous steps. We can further substitute the joint probability by the output distributions that we defined above:

$$\begin{aligned} &\log p(S_t|c, S_1...S_{t-1}) = \\ &- \log p(\text{types}_t|y_t^1) - \log p(\text{lat}_t, \text{lon}_t, \text{st}_t, \text{dur}_t|y_t^2) \end{aligned} \tag{26}$$

Put it together, we write the loss function give sequence and contextual information pair $(S, c)$ as the following:

$$\ell = \sum_{t=1}^{T} \Big[ - \log p(\text{types}_t|y_t^1) - \log p(\text{lat}_t, \text{lon}_t, \text{st}_t, \text{dur}_t|y_t^2) \Big] \tag{27}$$

# 4 Experiment Setup

## 4.1 Scenario micro-simulation

We describe the steps in a full-scale regional experiment where we train LSTM model for commuters from each of the 34 super-districts in the San Francisco Bay Area in order to develop an actionable mobility model for a typical weekday.

The data used in these studies comprise a month of anonymized and aggregated CDR logs collected in Summer 2015 by a major mobile carrier in the US, serving millions of customers in the San Francisco Bay Area. No personally identifiable information (PII) was gathered or used for this study. As described previously, CDR raw locations are converted into highly aggregated location features before any actual modeling takes places.

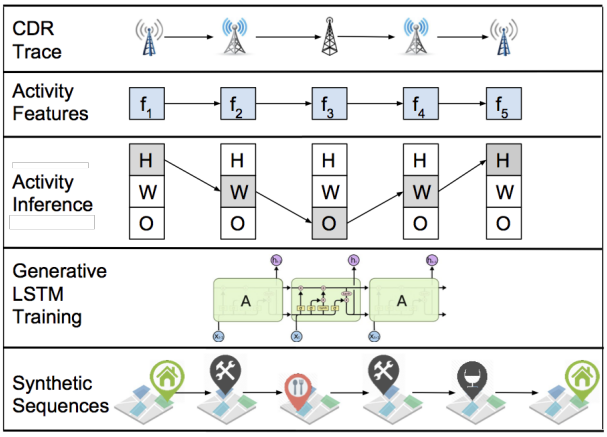


Figure 3: Processing of a CDR trace to synthetic activity sequence. Raw CDR traces are first converted to spatial and temporal feature sequences. Activity types were inferred from the spatial-temporal sequences.. Activity sequences with labels are sent to LSTM recurrent generative neural networks.

We pre-process the data following the steps in [30]. The home and work locations are identified during the pre-processing step using rule based classifier. We take cell phone users who showed up for more than 21 days a month at their identified "home" place; showed up for more than 14 days a month at their identified "work" place, and have home and work at different locations. These criteria identify regular working commuters

with a day structure containing both distinct Home and Work. The median number of activities is 4.4 per weekday and 4.0 per weekend. This is consistent with the California Household Travel Survey, reporting a number of 4 activities per day [1].

We tested our models' generative power in the Bay Area context. As travel patterns vary greatly over the region, we trained 34 LSTM models, each for a subset of cell phone users residing within each of the 34 super-districts as defined by the San Francisco Metropolitan Transportation Commission (MTC). We simulate 463,000 agents in the Bay Area (15% sample of the commuters) for each weekday: Monday through Friday.

# 5 Results

## 5.1 Scenario micro-simulation

This section describes the steps in a full-scale regional experiment where we train LSTM model for commuters from each of the 34 super-districts in the San Francisco Bay Area, in order to develop an actionable mobility model for a typical weekday.

The data used in these studies comprise a month of anonymized and aggregated CDR logs collected in Summer 2015 by a major mobile carrier in the US, serving millions of customers in the San Francisco Bay Area. No personally identifiable information (PII) was gathered or used for this study. As described previously, CDR raw locations are converted into highly aggregated location features before any actual modeling takes places.

We first present the temporal characteristics of the generated sequences in Fig. 4 and Fig. 5. From Monday to Friday, we observe a decreasing number of work and home activities while there is a slight increase in secondary (other) activities. Fig. 5 shows the joint distributions of starting time and duration of each activity type. The home activities starting around noon are relatively short. Night-time home activities have strong correlations between starting time and duration. Work activities show typical working patterns of commuters, while some last the entire day starting in the morning and others last only half of the day. Secondary (other) activities peak around the morning and afternoon commute hour, and they usually last within 1.5 hours. The temporal distributions are very similar to what is reported in other studies [30, 28].

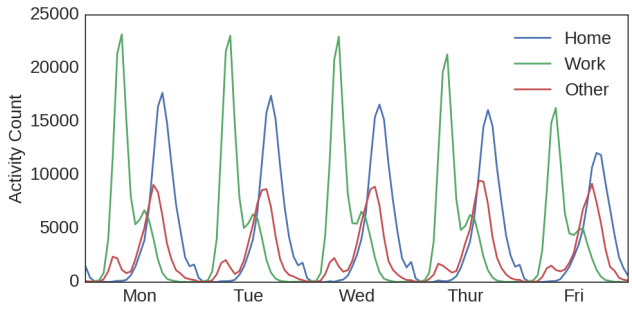


Figure 4: Number of activities (labeled per highest posterior probability) by their respective start time within a course of 5 weekdays.

Traffic micro-simulation is a conventional approach in studying performance and evaluating transportation planning and development scenarios, including the ones where the travel system conditions are changed and the response is extrapolated with behavioral models.

Micro-simulation of a typical weekday traffic is performed using the MATSim[1] platform [3]. MATSim is a state-of-the-art agent based multi-modal mobility micro-simulation tool that performs moe choice and traffic assignment for the set of agents with pre-defined activity plans. It varies departure times and routing of each agent depending on the congestion generated on the network, in order to maximize agent's daily utility, parametrically defined with several parameters including income, the value of time, and mode preference

[1]MATSim code available at `https://github.com/matsim-org`

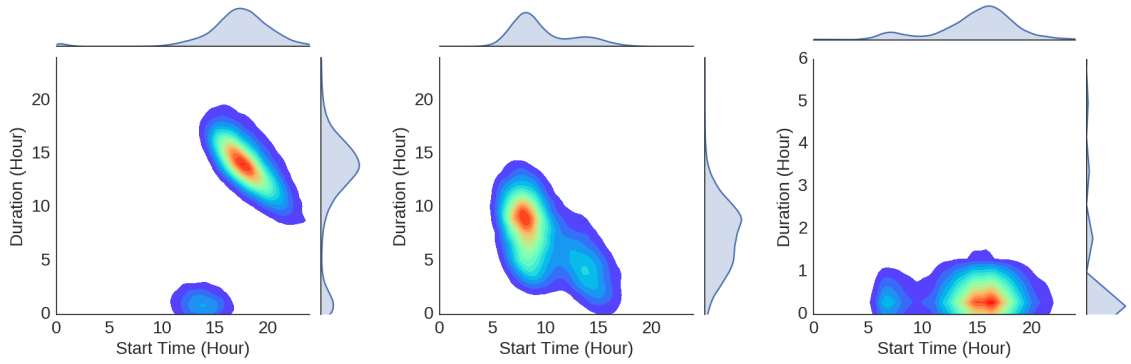


(a) Home (b) Work (c) Other Activities

Figure 5: Joint distribution plot of duration and start hour of labeled activities.

parameters. The simulation is run on the SF Bay Area network containing all major transit routes, freeways, primary and secondary roads (network fragment is visualized in Figure 6).

We have compared the results of the flows simulated from the generated activity sequences with the observed traffic and transit passenger volumes, provided by the California DOT Performance Management System (PeMS) and the Metropolitan Transportation Commission respectively. The simulation is run at 15% of the total population, and the road capacities as well as total resulting counts are scaled accordingly.

Note that observed traffic and transit passenger counts are not used for model calibration. They are used as independent data to evaluate the validity of the synthetic travel sequences produced with the LSTM model. Fig. 6 demonstrates examples of the three characteristic hourly volume profiles comparing the modeled and observed counts on freeways. Figure 7 shows examples of transit passengers counts entering and exiting 2 major rapid transit stations. Validation results for the full set of sensors are presented in Fig. 8. Fig. 8a shows a comparison of the volumes for three distinct time periods. Fig. 8b summarizes the validation results over 300 freeway and transit sensors in terms of the relative error (% volume) over-/under- estimated by the model as compared to the ground truth. One can notice lower accuracy at night and early morning hours explained by the fact that the model was developed and applied on a subset of daily commuters and did not include a large portion of trips performed by unemployed population and people working from home, besides multiple other traffic components (commercial fleets, taxis, visitors) that are out of scope of the model. Despite it's relative simplicity, the model has demonstrated a reasonable accuracy ($r^2 = 0.76, p < 10^{-3}$ in Fig. 8a ) as compared to the ground truth data.

# 6 Conclusions and Future Work

In this paper, we presented an end-to-end framework of modeling, and simulating urban mobility from cellular data. We proposed an LSTM model that is capable of learning explicit location choices that is applied on the labeled activity sequences. The LSTM model is also capable of learning activity trajectories with additional contextual information.

To examine the generative power of the LSTM model, we synthesized urban mobility plans using trained models. An agent-based micro-simulation of travel with multiple travel modes was run using the synthesized plans. The vehicle traffic counts and public transit boarding and alighting counts from the simulation result were compared with real traffic and transit data. A reasonable fit accuracy was observed. We also illustrated the results of using contextual information. LSTM models successfully learned the correlation between radius of gyration values and the corresponding trajectories. Both generated travel distances and generated radius of gyration showed such linear relationship to the contextual input. The LSTM also learned non-linear relationship between numerical income level and the activity trajectories. The generated distributions showed high similarity to the observed distributions in terms of radius of gyration and travel distance despite some discrepancies that can be observed.

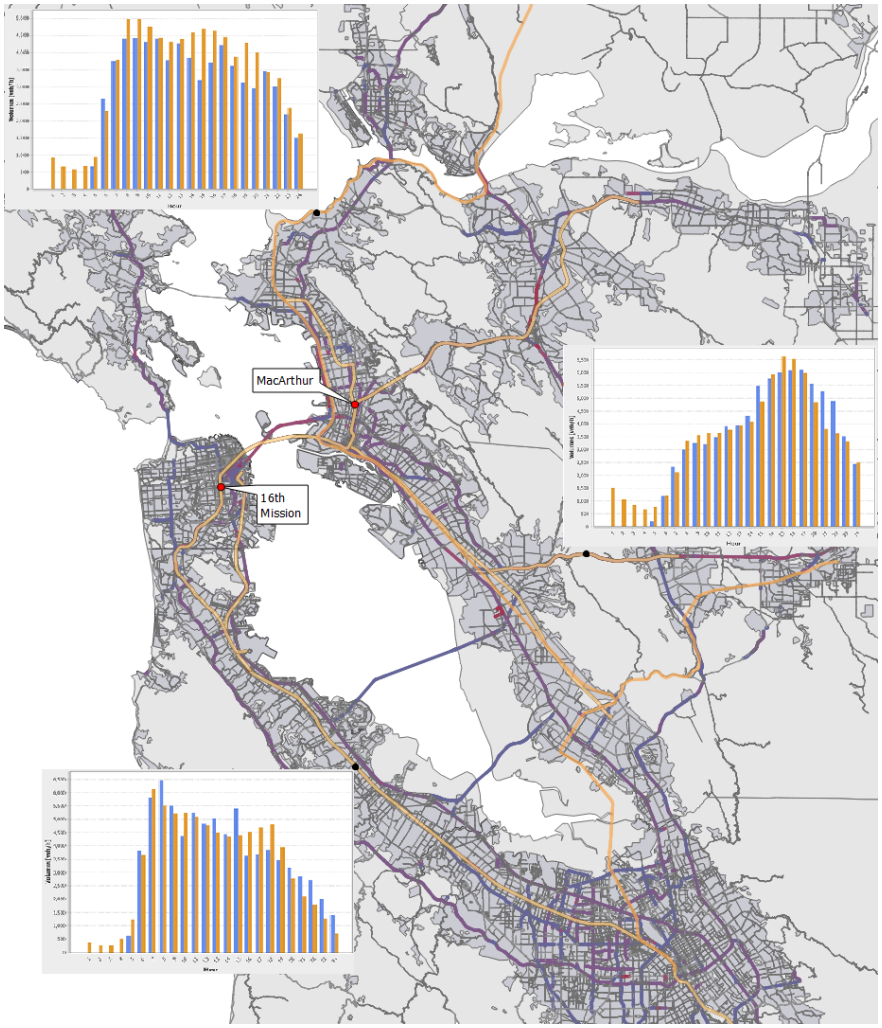


Figure 6: A fragment of the multi-modal SF Bay Area network with sample traffic volume detectors and transit stations used for validation. Inset graphs illustrate three sample hourly vehicle volume profiles for observed (orange) and modeled (blue) flows on a typical weekday in June 2015. Sample transit counts histograms are shown in Figure 7.

Traveling behavior is driven by complex decisions of individuals, which include attributes such as interpersonal interactions, in-home activities, and various other constraints. In this dissertation, the LSTM models we introduced focus on the modeling habits and patterns in stationary activities and trajectories of individuals. Part of the reason for our focus is the data sources. Locational data being the common data generated from mobile devices generally lacks information about the device owner and the decisions and attributes mentioned above. When further information becomes available, such as calendar information and social network connections, better modeling frameworks for more coherent traveling decisions can be developed with this additional information.

## Acknowledgments

This work was partially funded by a gift from AT&T. Support from the California DOT through UC-CONNECT program, agreement 65A0529, is also acknowledged. We thank Dr. Rashid Waraich and Andrew Campbell for their help in micro-simulation set up.

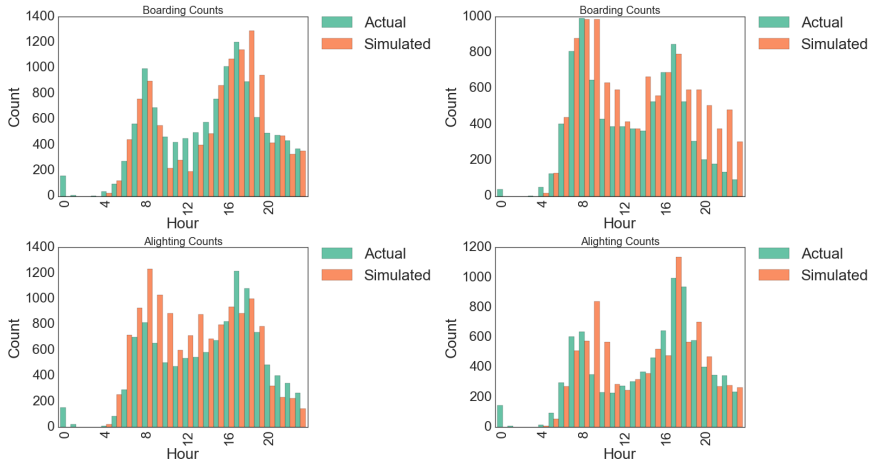


(a) 16th St. and Mission Station (b) MacArthur Station

Figure 7: Actual and simulated boarding and alighting counts on 2 major BART stations.

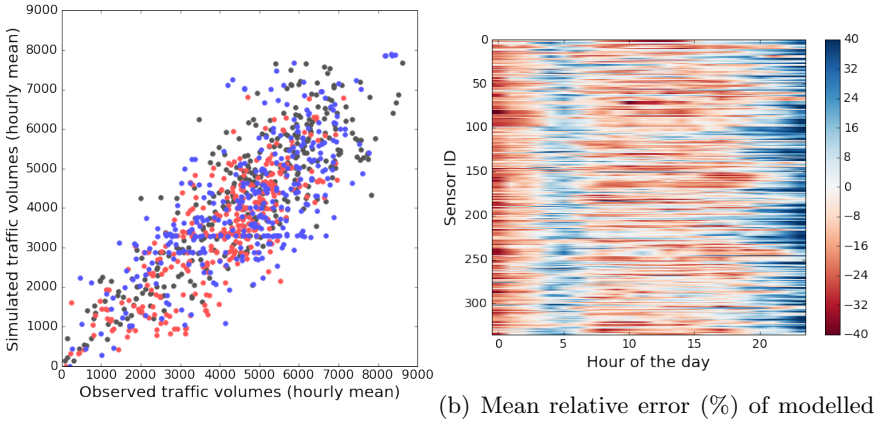


(a) Modeled vs observed volumes at 8am (black), 1pm (red) and 6pm (blue).

(b) Mean relative error (%) of modelled vs observed traffic volumes during the day.

Figure 8: Micro-simulation validation.

# References

[1] 2010-2012 california household travel survey final report appendix. `http://www.dot.ca.gov/hq/tpp/offices/omsp/statewide_travel_analysis/files/CHTS_Final_Report_June_2013.pdf`.

[2] A. Alahi, K. Goel, V. Ramanathan, A. Robicquet, L. Fei-Fei, and S. Savarese. Social lstm: Human trajectory prediction in crowded spaces. In *Proceedings of the IEEE Conference on Computer Vision and Pattern Recognition*, pages 961–971, 2016.

[3] M. Balmer, K. Meister, M. Rieser, K. Nagel, K. W. Axhausen, K. W. Axhausen, and K. W. Axhausen. *Agent-based simulation of travel demand: Structure and computational performance of MATSim-T*. ETH, Eidgenössische Technische Hochschule Zürich, IVT Institut für Verkehrsplanung und Transportsysteme, 2008.

[4] M. Ben-Akiva and B. Boccara. Discrete choice models with latent choice sets. *International Journal of Research in Marketing*, 12(1):9–24, 1995.

[5] C. M. Bishop. Mixture density networks. 1994.

[6] C. C. Cantarelli, B. Flyvbjerg, E. J. Molin, and B. van Wee. Cost overruns in large-scale transportation infrastructure projects: explanations and their theoretical embeddedness. 2010.

[7] C. Chen, J. Ma, Y. Susilo, Y. Liu, and M. Wang. The promises of big data and small data for travel behavior (aka human mobility) analysis. *Transportation Research Part C: Emerging Technologies*, 68:285–299, 2016.

[8] E. Cho, S. A. Myers, and J. Leskovec. Friendship and mobility: user movement in location-based social networks. In *Proceedings of the 17th ACM SIGKDD international conference on Knowledge discovery and data mining*, pages 1082–1090. ACM, 2011.

[9] J. Chung, K. Kastner, L. Dinh, K. Goel, A. C. Courville, and Y. Bengio. A recurrent latent variable model for sequential data. In *Advances in neural information processing systems*, pages 2980–2988, 2015.

[10] C. Cottrill, F. Pereira, F. Zhao, I. Dias, H. Lim, M. Ben-Akiva, and P. Zegras. Future mobility survey: Experience in developing a smartphone-based travel survey in singapore. *Transportation Research Record: Journal of the Transportation Research Board*, (2354):59–67, 2013.

[11] H. Dai, B. Dai, Y.-M. Zhang, S. Li, and L. Song. Recurrent hidden semi-markov model. 2016.

[12] P. Deville, C. Linard, S. Martin, M. Gilbert, F. R. Stevens, A. E. Gaughan, V. D. Blondel, and A. J. Tatem. Dynamic population mapping using mobile phone data. *Proceedings of the National Academy of Sciences*, 111(45):15888–15893, 2014.

[13] B. Flyvbjerg, N. Bruzelius, and W. Rothengatter. *Megaprojects and risk: An anatomy of ambition*. Cambridge University Press, 2003.

[14] M. C. Gonzalez, C. A. Hidalgo, and A.-L. Barabasi. Understanding individual human mobility patterns. *Nature*, 453(7196):779–782, 2008.

[15] A. Graves. Generating sequences with recurrent neural networks. *arXiv preprint arXiv:1308.0850*, 2013.

[16] K. Gregor, I. Danihelka, A. Graves, D. J. Rezende, and D. Wierstra. Draw: A recurrent neural network for image generation. *arXiv:1502.04623*, 2015.

[17] R. Hariharan and K. Toyama. Project lachesis: parsing and modeling location histories. In *Geographic Information Science*, pages 106–124. Springer, 2004.

[18] S. Hochreiter and J. Schmidhuber. Long short-term memory. *Neural computation*, 9(8):1735–1780, 1997.

[19] F. Kling and A. Pozdnoukhov. When a city tells a story: urban topic analysis. In *Proceedings of the 20th international conference on advances in geographic information systems*, pages 482–485. ACM, 2012.

[20] L. Liao, D. Fox, and H. Kautz. Hierarchical conditional random fields for gps-based activity recognition. In *Robotics Research*, pages 487–506. Springer, 2007.

[21] X. Lu, L. Bengtsson, and P. Holme. Predictability of population displacement after the 2010 haiti earthquake. *Proceedings of the National Academy of Sciences*, 109(29):11576–11581, 2012.

[22] C. Song, Z. Qu, N. Blumm, and A.-L. Barabási. Limits of predictability in human mobility. *Science*, 327(5968):1018–1021, 2010.

[23] X. Song, H. Kanasugi, and R. Shibasaki. Deeptransport: Prediction and simulation of human mobility and transportation mode at a citywide level. IJCAI, 2016.

[24] I. Sutskever, J. Martens, and G. E. Hinton. Generating text with recurrent neural networks. In *Proceedings of the 28th International Conference on Machine Learning (ICML-11)*, pages 1017–1024, 2011.

[25] I. Sutskever, O. Vinyals, and Q. V. Le. Sequence to sequence learning with neural networks. In *NIPS*, pages 3104–3112, 2014.

[26] US Department of Transportation: Federal Transit. The Predicted and Actual Impacts of New Starts Projects - 2007: Capital Cost and Ridership. Technical report, 2008.

[27] P. Wang, T. Hunter, A. M. Bayen, K. Schechtner, and M. C. González. Understanding road usage patterns in urban areas. *Scientific reports*, 2, 2012.

[28] P. Widhalm, Y. Yang, M. Ulm, S. Athavale, and M. C. González. Discovering urban activity patterns in cell phone data. *Transportation*, 42(4):597–623, 2015.

[29] J. Ye, Z. Zhu, and H. Cheng. What's your next move: User activity prediction in location-based social networks. In *Proceedings of the SIAM International Conference on Data Mining. SIAM*, 2013.

[30] M. Yin, M. Sheehan, S. Feygin, J.-F. Paiement, and A. Pozdnoukhov. A generative model of urban activities from cellular data. *IEEE Transactions in ITS*.

[31] C. Zhang, K. Zhang, Q. Yuan, L. Zhang, T. Hanratty, and J. Han. Gmove: Group-level mobility modeling using geo-tagged social media. In *Proceedings of the 22nd ACM SIGKDD International Conference on Knowledge Discovery and Data Mining*, pages 1305–1314. ACM, 2016.

[32] Y. Zheng, L. Capra, O. Wolfson, and H. Yang. Urban computing: concepts, methodologies, and applications. *ACM Transactions on Intelligent Systems and Technology (TIST)*, 5(3):38, 2014.

[33] Y. Zheng, Q. Li, Y. Chen, X. Xie, and W.-Y. Ma. Understanding mobility based on gps data. In *Proceedings of the 10th international conference on Ubiquitous computing*, pages 312–321. ACM, 2008.

[34] W.-Y. Zhu, W.-C. Peng, L.-J. Chen, K. Zheng, and X. Zhou. Modeling user mobility for location promotion in location-based social networks. In *Proceedings of the 21th ACM SIGKDD International Conference on Knowledge Discovery and Data Mining*, pages 1573–1582. ACM, 2015.